

# Determination of the Stability of pit slope of the Opencast Coal Mines Workings by Underground Mining

Gopal Rajak<sup>1\*</sup> and Hemant Kumar<sup>2</sup>

<sup>1</sup>Research Scholar, Indian Institute of Technology, Indian School of Mines, Dhanbad, Jharkhand-826004,  
E-mail: [gopal.16dr000239@me.ism.ac.in](mailto:gopal.16dr000239@me.ism.ac.in)

<sup>2</sup>Assistant Professor, Indian Institute of Technology, Indian School of Mines, Dhanbad, Jharkhand-826004,  
Email: [hemant@iitism.ac.in](mailto:hemant@iitism.ac.in)

## Abstract

Long back, underground mining was continued in the shallow depth. Huge quantities of coal were lost due to the improper method and unavailability of the types of machinery. The technological evaluation is again a big change with a higher stripping ratio, and opencast mining has played a significant role in the coal extraction in the greater depth. The pillar left in the shallow depth underground mining again has been taken out by opencast mining. This paper examines the effect of developed underground workings on the stability of the opencast slope. It compares the various parameters like critical Strength Reduction Factor (SRF), total displacement and maximum shear strain. The study shows that the safety of the slope made on standing pillars/developed galleries is less than a slope made on virgin strata. Hence, the mining engineers need to account for the reduction in factor of safety and plan the slope angle accordingly. Every parameter, such as overall slope angle, depth of underground workings, internal angle of friction, the width of gallery and pillars of underground workings, have a significant role in determining the factor of safety. In a parametric study, the critically dependent parameter is examined with regression analysis to calculate the safety factor in such cases. This paper may help to decide the bench height and slope angle in the opencast mining.

**Keywords:** Opencast mining, Development, Numerical Modelling, Coal mining, Pit Slope

## 1.0 Introduction

Slope stability analysis has been carried out by many researchers worldwide, which mostly involves the traditional limit equilibrium method due to its simplicity and easy to use. The limit equilibrium has its disadvantage like assumptions of shape, location and direction of failure, and it becomes inadequate if the slope fails due to complex mechanisms (e.g. internal deformation, strain localisation, progressive creep, liquefaction of weaker material layers etc.). Krahn, 2003

asserted that “it is the absence of a stress–strain relationship in conventional limit equilibrium analysis methods that is the fundamental piece of missing physics.” The finite element method has emerged as a powerful tool which can be used to analyse slope stability with complex shapes without any prior assumptions. The information about deformations can be obtained and can monitor progressive failure, including overall shear failure (Griffiths & Lane, 2001). Another demerit of limit equilibrium is when the slopes with excavated boundaries must be analysed, while finite element software like Phase 2, ANSYS, and Diana can successfully model these conditions, limit equilibrium software fails to do so. Deliveries

\*Author for correspondence

and Zevgolis, 2016 studied the comparative performance between finite element method (FEM) and finite difference (FDM) method employing two FEM softwares (PLAXIS, PHASE2) and FDM software (FLAC) by simulating a slope of an open pit mine. It was concluded that all three programs can model the problem satisfactorily. Hence in this study Phase 2 software is used for analysis. Due to the advancement in opencast technology, increased safety and low labour-intensive process, there has been a shift from the underground mine to open pit mines. These shifts have caused new opencast mines issues, like working opencast mines over previously mined bord and pillar underground methods. There have been growing concerns over the factor of safety of slopes made in these opencast mines, as local failures can be seen over these workings (Figure 3). It is very important to consider the effect of these working to predict a safe slope angle which would not fail throughout its designed life.

## 2.0 Shear Strength Reduction Method

In the conventional Limit Equilibrium method, the critical slip surface has to be determined and the average shear strengths along the slip surface are treated the same. The factor of safety (FoS) used in the LE method is defined as the ratio of the average shear strength to the driving shear stress along the potential slip surface. However, the potential slip surface in the FE analysis need not be determined in advance. The finite element analysis is conducted on every element for the developed stress, strain and deformation, but it cannot directly output a global factor of safety. In order to quantify an equivalent FoS from the LE methods, the strength reduction method (Nianet al. 2012; Zhang et al. 2013) is employed. The shear strength reduction (SSR) method, also known as the strength reduction method (SRM), has gained popularity among researchers for slope stability analysis in the finite element method. Many researchers have documented the method (Zienkiewicz 1975; Matsui and San 1992; Griffiths and Lane 1999, Stiansonet al. 2011; Nianet al. 2012; Zhang et al. 2013). The strength reduction factor (SRF) is applied to reduce the material strength until the solution fails to converge.

### 2.1 Methodology of Strength Reduction

The strength parameters are reduced by a certain factor known as (SRF), and the finite element stress analysis is computed. This process is repeated for different values of strength reduction factor (SRF) until the model becomes unstable, i.e. the analysis results do not converge. The SRF at which analysis fails to converge is known as the critical

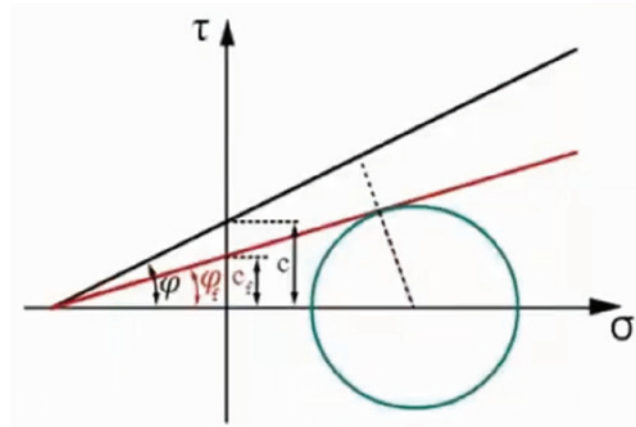


Figure 1(a): Representation of SRF on Mohr's Circle

strength reduction factor (critical SRF) or safety factor of the slope. The methodology is explained in Fig.1b:

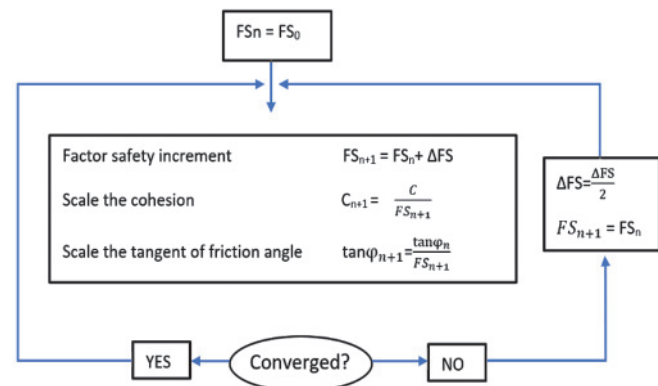


Figure 1(b): Strength reduction methodology

## 3.0 Description of the Study Mine – A Case Study

In this paper slope of a mine is modelled using finite element software for different values of overall slope angle, depth of UG workings, internal angle of friction, gallery width and pillars of underground workings. The mine has been developed using the bord and pillar method around 25 years back, which is now being mined using the opencast method. The plans for the underground work were made a long time ago. So, these plans have deteriorated. Moreover, the correctness of these plans remains questionable. However, the available plans and sections were studied in detail to make the model.

The study area is located in the western part of the Jharia coalfield in the Dhanbad district of Jharkhand State, under the jurisdiction of BCCL. The project has a leasehold area of 731.35 ha with latitude 23°46'00"N to 23°48'24"N and longitude

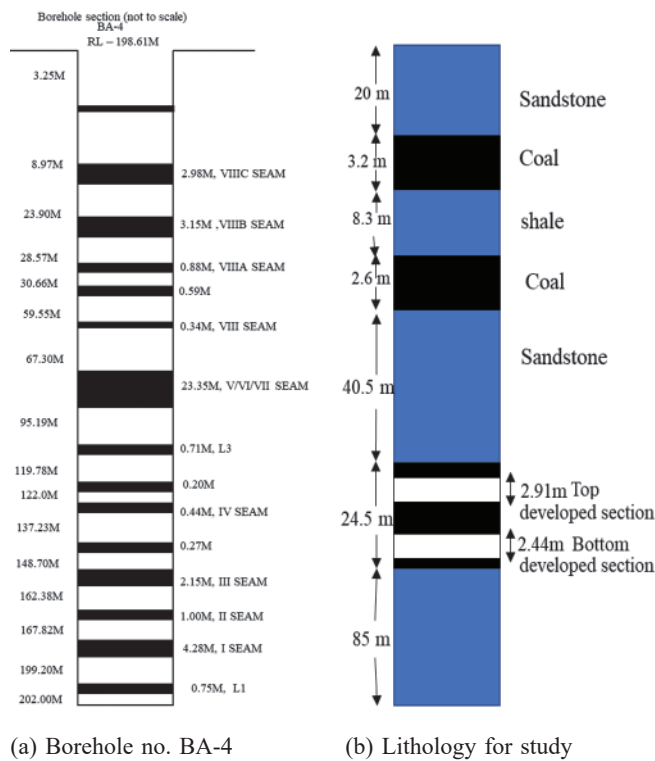


Figure 2: Key borehole data and lithology of mine site used for numerical modelling



Figure 3(a): Old developed galleries are being seen in the opencast bench

86°12'45"E to 86°15'24" E. Total eight numbers of coal seams exist in the leasehold area, namely I, II, III, IV, V/VI/VII (combined), VIII A, VIII B and VIII C seam and these seams are lying in the ascending. The present working depth of the mine is around 90mts, and working is progressing in the seam V/VI/VII (combined). The thickness of the seam varies from 22 m to 28m. The average thickness of this seam is 24.5m and is already developed with bottom and top sections considering a 9.65m parting. The top section lies at 5.5m below the roof of the seam, and the bottom section lies at 4m from the floor of the seam. The height of the top and bottom

sections are 2.91m and 2.44m, respectively, as shown in Figure 2.

Figure 2 shows the lithology of the mine site and is used for developing the 2D finite element model in Phase 2 software. Figure 3 shows the typical old workings that exist on the highwall/slope of the bench, and the local failure has also occurred over the bench during September 2020.

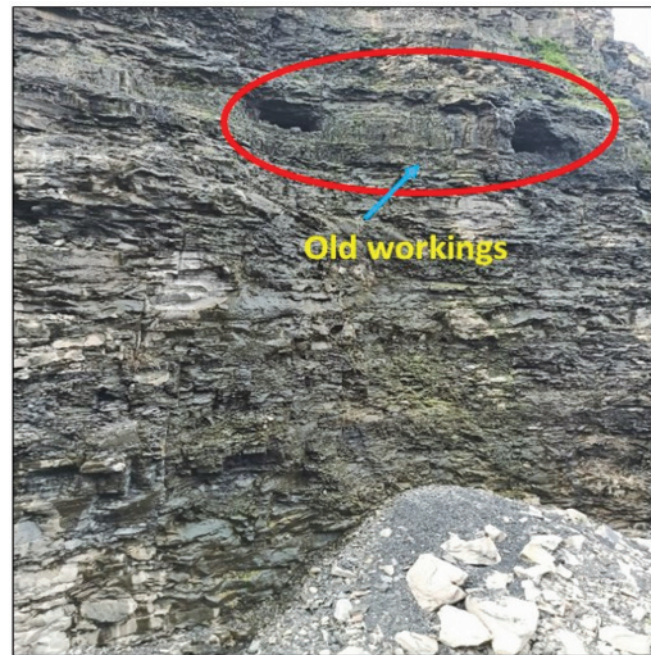


Figure 3(b): Local failure observed around old developed galleries.

### 3.1 Material Properties

Rockmass rating of the coal seam, sandstone and shale are 55, 62 and 59 respectively. The intact rock properties of the mine site are collected from the mine site and are converted to rockmass properties using Hoek-Brown rock media (Islavath and Deb, 2018). Rockmass properties such as modulus of elasticity (E), Unit Weight ( $\gamma$ ), poisson's ratio ( $\nu$ ), Tensile strength ( $\sigma_t$ ), Cohesion (C), Friction angle ( $\phi$ ) and Dilation angle ( $\psi$ ) used in the finite element modelling are listed in Table 1. Elastic isotropic material with Mohr-coulomb failure criteria is used for the analysis.

### 4.0 Development of the Model

The current mine plan of opencast mine and the projections of underground working on the plan are studied. One model is made from actual mine details, as shown in Figure 4. Then 431 variations of the model are created by changing the height of the models 345m, 365m, 385m to 405m, overall slope angle 26°, 36°, 46° and 56°, pillar width -13m, 20m and 27m,

**Table 1: Rockmass properties**

Property	Value for Sandstone	Value for Coal
Young's Modulus E (MPa)	5000	2000
Poisson's ratio, $\nu$	0.028	0.3
Unit Weight, $\gamma$ (MN/m <sup>3</sup> )	0.023	0.016
Tensile strength (MPa)	2	1
Cohesion (MPa)	0.13	0.08
Friction angle (deg)	30	25
Dilation angle (deg)	0	0

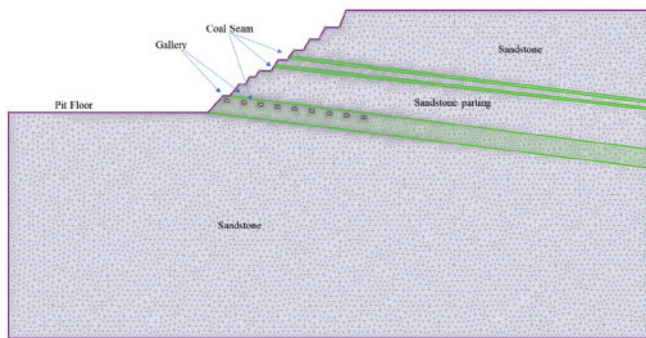


Figure 4: Mesh of the model in Phase 2

gallery width-3m, 3.6m and 4.8m and friction angle (Coal/OB)-15/20°, 20/25° and 25/30°. The width of the model is 757m for all the cases. A total of 432 models were created with UG workings and 16 models in virgin strata and factor of safety calculated for all the model using shear strength reduction method.

### 4.1 Validation of the model

Factor of safety of the slope is calculated using different methods like Ordinary/Fellenius, Bishop simplified, Janbu simplified, Janbu corrected, Spencer and Phase 2 (finite element). The results are plotted in Figure 5, it can be seen

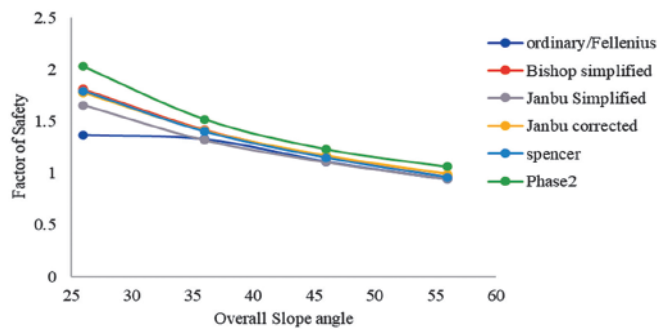


Figure 5: FoS using various methods

that there are larger variations in FoS for 26° but as we move towards higher slope angle the factor of safety calculated using Phase 2 and other methods fall in line with each other. So, the model can be successfully used to predict the behaviour of slope. However it should be noted that the FoS using Phase 2 are slightly higher than other methods. Since the other methods are not suitable for finding FoS of slope with developed UG working the comparison is made only for slope in virgin strata.

## 5.0 Results and Discussions

### 5.1 Single Developed Section Versus Multiple Developed Sections

The study area has a seam named V/VI/VII (combined) developed in two sections as discussed above. Initially, a comparative study was done, and the simulations were run considering both single and multiple developed sections, as shown in Figures 6 and 7. However, it was observed from Figure 8 that the factor of safety decreases sharply when compared to virgin strata and developed UG workings but when correlation is made between a single section and multiple sections, the difference was not significant as compared to the virgin strata. So, further studies were conducted for single workings only.

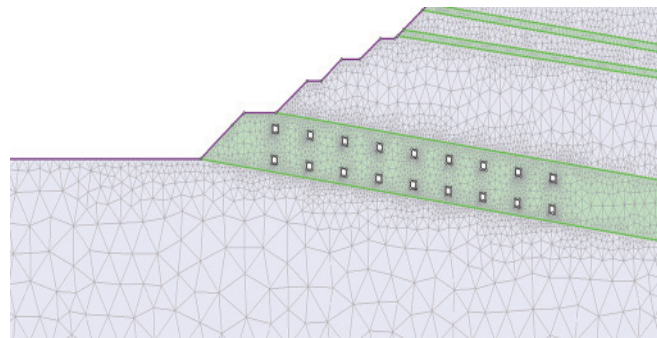


Figure 6: A model consisting of two developed section

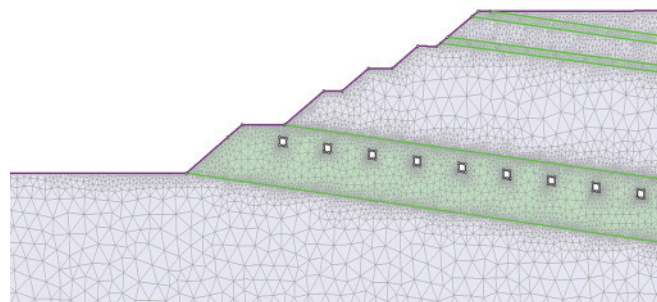


Figure 7: A model consisting of a single developed section

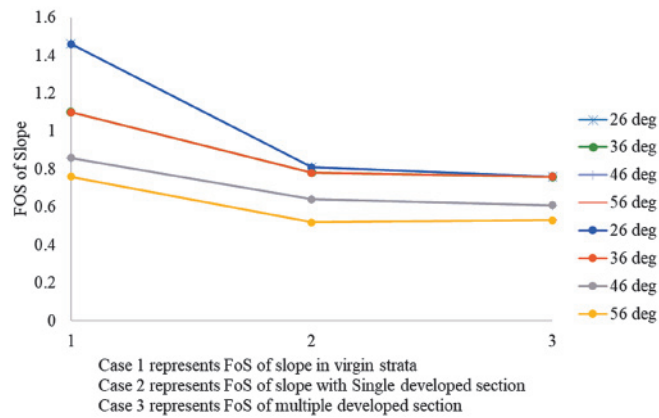


Figure 8: Factor of safety of slope in virgin strata, single and multiple developed workings

### 5.2 Effect of Internal Angle of Friction on FoS

From Figure 9, it is observed that the difference in factor of safety for lower friction angle values is less than the larger friction angle. For a friction angle of 10°, the difference is 0.17; however, for 50°, it is 0.79. The slope of curve for both cases increases with the increase in friction angle.

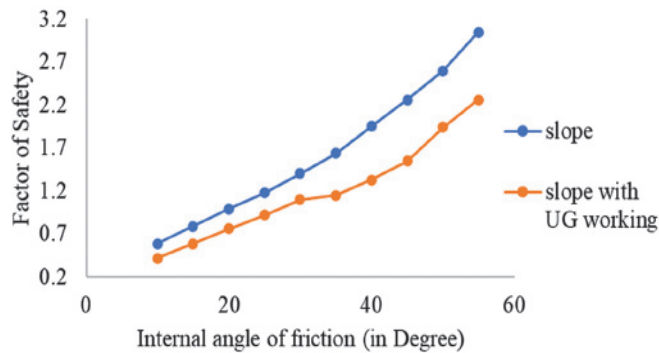


Figure 9: Effect of internal angle of friction

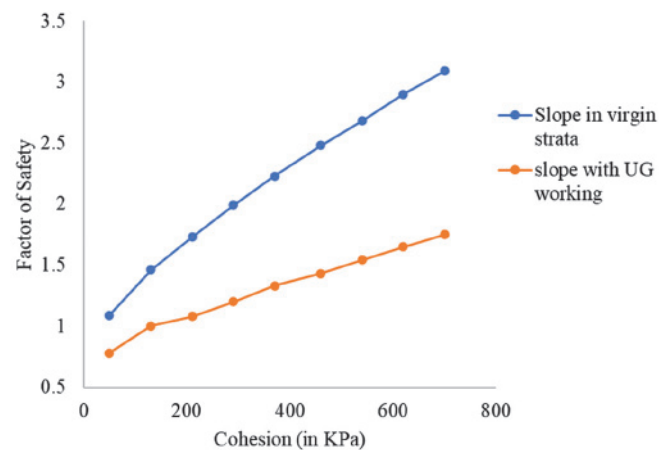


Figure 10: Effect of Cohesion

### 5.3 Effect of Cohesion on FoS

It can be seen from the Figure 10 that for the cohesion of 130 KPa, the difference in FoS is 0.46, while for the cohesion of 800 KPa, the difference is 1.34. Here, the slope of the curve decreases with the increase in cohesion.

### 5.4 Effect of Unit Weight on FoS

With the increase in unit weight, the FoS decreases; however, the difference in factor of safety for both the cases remains the same unlike with internal angle of friction and cohesion.

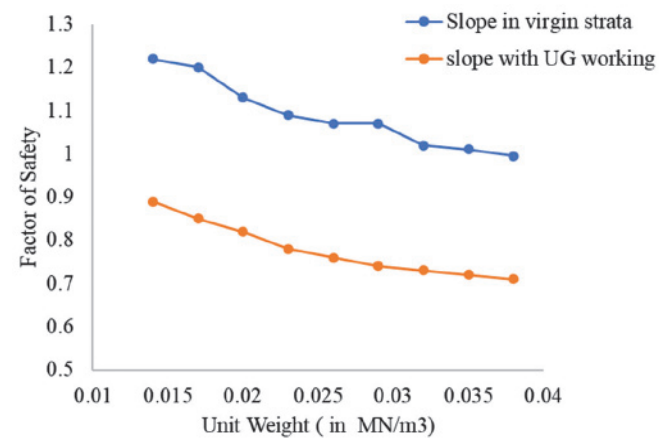


Figure 11: Effect of Unit weight

### 5.5 Maximum Shear Strain

Figures 15 through 18 show the maximum shear strain distribution observed in pit slopes as the slope angle varies from 26° to 56°. There is a sharp increase in the value of maximum shear strain in the case of underground workings as compared to the slopes made on virgin seams. The maximum shear strain in the 26° slope is 0.03, while in the 26° slope with UG working, it is 0.4. The same trend continues with other models, i.e., in the case of the slope with 36°, it increases from 0.03 to 0.4, in 46° slope, it increases from 0.019 to 0.05, and in the case of 56°, the increase is from 0.011 to 0.030. Also, in the case of slopes made on virgin seams, the failure path is easily visible, but in slopes with UG working failure path is not easily seen in all the cases; however, it may be seen in a few cases of slopes with angle 56° as shown in Figures 12, 13 and 14.

As mentioned earlier failure path is difficult to observe because the stress get concentrated over the galleries, and during the study, it was observed on slopes with 56°, which are plotted in Figures 12 through 14. These figures show the progressive failure paths as the strength reduction process continues for the critical SRF 1.05 in the software.

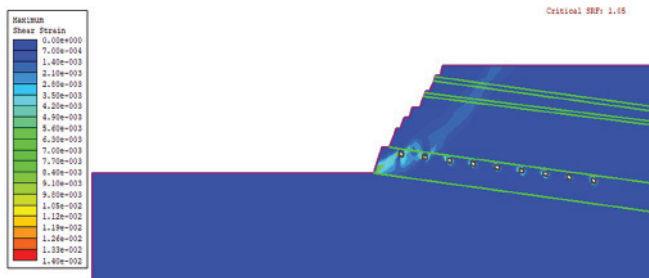


Figure 12: Failure path observed for SRF 1.05 for  $\theta=56^\circ$  H=80m P=20m W=3.6m

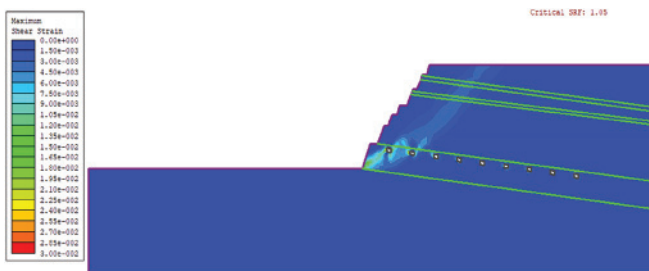


Figure 13: Failure path observed for SRF 1.09 for  $\theta=56^\circ$  H=80m P=20m W=3.6m

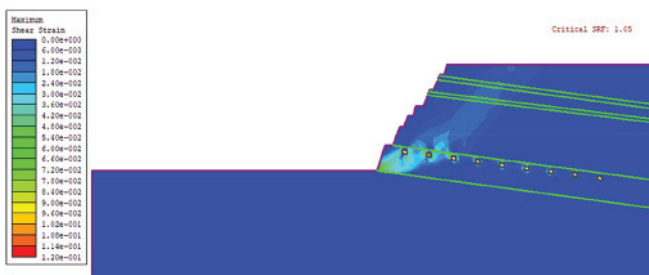


Figure 14: Failure path observed for SRF 1.2 for  $\theta=56^\circ$  H=80m P=20m W=3.6m

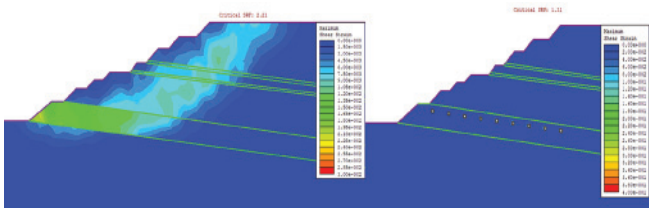


Figure 15: Maximum shear strain distribution for  $\theta=26^\circ$ , H=100m, P=20m, W=3m

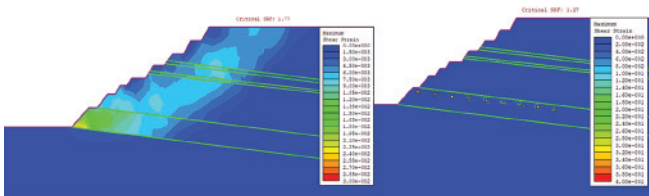


Figure 16: Maximum shear strain distribution for  $\theta=36^\circ$ , H=100m, P=20m, W=3m

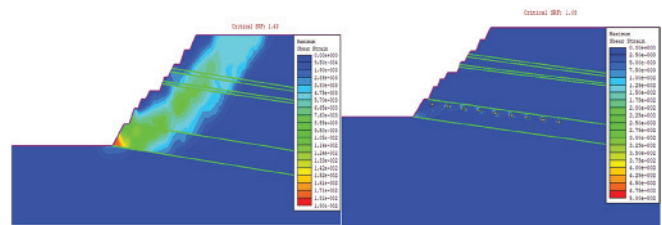


Figure 17: Maximum shear strain distribution for  $\theta=46^\circ$ , H=100m, P=20m, W=3m

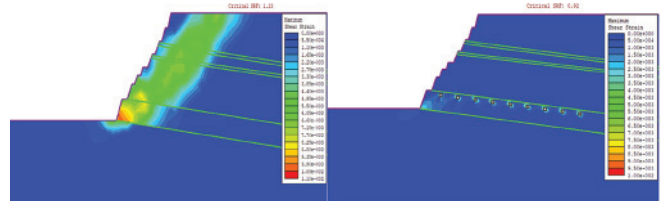


Figure 18: Maximum shear strain distribution for  $\theta=56^\circ$ , H=100m, P=20m, W=3m

## 5.6 SRF/FoS

Figures 15 to 18 show comparative results when the slope angle varies gradually from  $26^\circ$  to  $56^\circ$ . All the slopes were stable if underground workings were not present, but the analysis in the presence of underground working shows that the factor of safety of slope with an angle of  $46^\circ$  decreases from 1.43 to 1.08 and that of the slope with an angle of  $56^\circ$  decreases from 1.23 to 0.92. Generally, for the safe design of pit slope, a factor of safety of 1.2 is considered to be a good estimation. From the above analysis, it is clear that the slope with angles of  $46^\circ$  and  $56^\circ$  were stable without UG working, but in the presence of UG working, both the slope fails.

## 6.0 Conclusions

Previously worked underground workings affect the stability of opencast mines that are being worked over these workings. The FoS of slopes on virgin strata, when compared to the FoS of single developed section and multiple developed sections, gives a substantial difference, but when a single developed section is compared to a double section, this does not provide a significant difference.

With the increase in friction angle, the FoS increases, but the rate of increase is less in slope with the developed gallery. For a friction angle of  $10^\circ$ , the difference in FoS for both cases is 0.17; however, for  $50^\circ$ , it is 0.79.

With the increase in cohesion, the FoS also increases, but the amount of increase is less in the case of developed galleries. For the cohesion of 130 KPa, the difference in FoS is 0.46, while for the cohesion of 800 KPa, the difference is 1.34.

With the increase in unit weight, the FoS decreases; however, the difference in factor of safety for both the cases remains the same, unlike with internal angle of friction and cohesion, where the amount increases or decreases varies.

The maximum shear strain in the 26° slope is 0.03, while in the 26° slope with UG working, it is 0.4. The same trend continues with other models, i.e., in the case of the slope with 36°, it increases from 0.03 to 0.4, in the 46° slope, it increases from 0.019 to 0.05, and in the case of 56°, the increase is from 0.011 to 0.030.

## 7.0 Acknowledgements

The authors are thankful to the management of various mines of Coal India Limited, who provided logistic support and necessary information for conducting field studies and collecting various rock samples. This study forms a part of the ongoing doctoral research of the author. The views expressed in this paper are those of the authors and not necessarily of the organisation to which they belong.

Funding : The author(s) received no financial support for this article's research, authorship, and/or publication.

Conflict of interest: The authors declare that they have no conflict of interest.

## 8.0 Reference

- Chen, B. (2017). Finite element strength reduction analysis on slope stability based on ANSYS. *Environmental and Earth Sciences Research Journal*, 4(3), 60–65. <https://doi.org/10.18280/eeerj.040302>
- Fawaz, A. (2014). Slope Stability Analysis Using Numerical Modelling. *American Journal of Civil Engineering*, 2(3), 60. <https://doi.org/10.11648/j.ajce.20140203.11>
- Fawaz, A., Farah, E., & Hagechade, F. (2014). Slope Stability Analysis Using Numerical Modelling. [Http://www.sciencepublishinggroup.com](http://www.sciencepublishinggroup.com), 2(3), 60. <https://doi.org/10.11648/J.AJCE.20140203.11>
- Griffiths, D. v., & Lane, P. A. (2001). Slope stability analysis by finite elements. *Géotechnique*, 51(7), 653–654. <https://doi.org/10.1680/geot.51.7.653.51390>
- Griffiths, D.V. and Lane, P.A. (1999). "Slope stability analysis by finite elements." *Géotechnique*, 49(3), 387-403.
- Hammah, R. E., Curran, J. H., & Yacoub, T. (2004). Stability Analysis of Rock Slopes using the Finite Element Method.
- Ho, I. H. (2014): Parametric studies of slope stability analyses using three-dimensional finite element technique: Geometric effect. *Journal of GeEngineering*, 9(1), 33–43. [https://doi.org/10.6310/JOG.2014.9\(1\).4](https://doi.org/10.6310/JOG.2014.9(1).4)
- Islavath S R, Deb DebasisD. Stability analysis of underground stope pillars using three-dimensional numerical modelling techniques. *Int. J. Mining and Mineral Engineering*. 2018;9(3):198-215.
- Matsui, T. and San, K.C. (1992). "Finite element slope stability analysis by shear strength reduction technique." *Soils and Foundations*, 32(1), 59-70.
- Ngwenyama, P. L., & de Graaf, W. W. (2021). Risks and challenges affecting opencast pillar mining in previously mined underground bord and pillar workings. *The Journal of the Southern African Institute of Mining and Metallurgy*, 121. <https://doi.org/10.17159/2411>
- Nian, T.K., Huang, R.Q., Wan, S.S., and Chen, G.Q. (2012). "Three-dimensional strength-reduction finite element analysis of slopes: Geometric effects." *Canadian Geotechnical Journal*, 49(5), 574-588.
- Pal Roy, P., Sawmliana, C., Prakash, A., & Singh, R. K. (2020). Safe exploitation of developed pillars of a coal seam above fire affected areas—a case study. *Mining Technology: Transactions of the Institute of Mining and Metallurgy*, 129(4), 206–216. <https://doi.org/10.1080/25726668.2020.1834972>
- Rocscience Inc. (2004). Application of the Finite Element Method to Slope Stability. Rocscience.
- Saha, S. (n.d.). Indian Geotechnical Conference-2010.
- Satyanarayana, I., Budi, G., & Murmu, S. (n.d.). Stability analysis of a deep highwall slope using numerical modelling and statistical approach—a case study. <https://doi.org/10.1007/s12517-021-06476-x>Published
- Stianson, J.R., Fredlund, D.G., and Chan, D. (2011). "Three-dimensional slope stability based on stresses from a stress deformation analysis." *Canadian Geotechnical Journal*, 48.
- Zhang, Y., Chen, G., Zheng, L., Li, Y., and Zhuang, X. (2013). "Effects of geometries on three-dimensional slope stability." *Canadian Geotechnical Journal*, 50, 233-249.
- Zienkiewicz, O.C., Humpheson, C., and Lewis, R.W. (1975) "Associated and non-associated viscoplasticity and plasticity in soil mechanics." *Géotechnique*, 25(4), 671-689.